



PERGAMON

Available online at www.sciencedirect.com

SCIENCE @ DIRECT®

INTERNATIONAL JOURNAL OF

NON-LINEAR
MECHANICS

www.elsevier.com/locate/nlm

International Journal of Non-Linear Mechanics 39 (2004) 491–502

Perturbation solution for secondary bifurcation in the quadratically-damped Mathieu equation

Deepak V. Ramani^{a,*}, William L. Keith^a, Richard H. Rand^b

^aNaval Undersea Warfare Center, Newport, RI 02841, USA

^bDepartment of Theoretical and Applied Mechanics, Cornell University, Ithaca, NY 14853, USA

Received 13 December 2001; accepted 1 October 2002

Abstract

This paper concerns the quadratically-damped Mathieu equation:

$$\ddot{x} + (\delta + \varepsilon \cos t)x + \dot{x}|\dot{x}| = 0.$$

Numerical integration shows the existence of a secondary bifurcation in which a pair of limit cycles come together and disappear (a saddle-node of limit cycles). In δ - ε parameter space, this secondary bifurcation appears as a curve which emanates from one of the *transition curves* of the linear Mathieu equation for $\varepsilon \approx 1.5$. The bifurcation point along with an approximation for the bifurcation curve is obtained by a perturbation method which uses Mathieu functions rather than the usual sines and cosines.

Published by Elsevier Ltd.

Keywords: Nonlinear; Mathieu; Perturbation; Bifurcation; Resonance

1. Introduction

The Mathieu equation

$$\ddot{x} + (\delta + \varepsilon \cos t)x = 0 \quad (1)$$

is a well-known example of a linear differential equation with periodic coefficients. The stability properties of the Mathieu equation may be obtained by the use of Floquet theory; see [1]. A survey of some of the non-linear variations of the Mathieu equation has been presented in [2].

The quadratically-damped Mathieu equation,

$$\ddot{x} + (\delta + \varepsilon \cos t)x + \dot{x}|\dot{x}| = 0, \quad (2)$$

which is studied here, has application to the dynamics of passive towed arrays in submarines. The physical application and the derivation of the equation has been detailed in [3,4]. In addition to deriving the quadratically-damped Mathieu equation, the previous works carried out a linear stability analysis as well as a small- ε non-linear stability analysis via the method of averaging. These works also contained an incomplete analytical treatment of the secondary bifurcation. The objective of the present work is to complete the analytical treatment of the secondary bifurcation, to determine the nature of the bifurcation, and to approximate the bifurcation curve.

* Corresponding author.

E-mail address: ramanidv@npt.nuwc.navy.mil (D.V. Ramani).

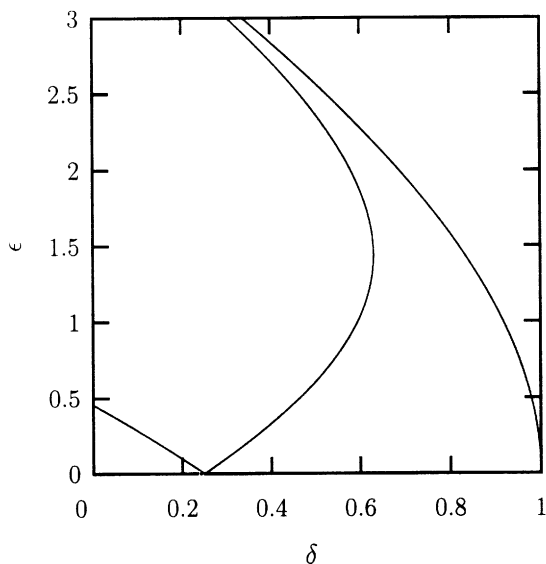


Fig. 1. Transition curves of the linear Mathieu equation.

2. Linear stability and small ε results

Eq. (2) admits the exact solution $x \equiv 0$. The stability of this solution is governed by the linear Mathieu equation, Eq. (1). The origin is considered *stable* if all solutions of Eq. (1) are bounded, and *unstable* if an unbounded solution exists. The stability treatment of Eq. (1) demonstrates the existence of regions in the δ - ε plane, called *tongues*, which emanate from the δ -axis at points $\delta = n^2/4$, where $n = 0, 1, 2, 3, \dots$ [1]. Inside the tongues, the origin is unstable, while outside the tongues, the origin is stable. The tongues of instability are said to be bounded by *transition curves*. Because the linear Mathieu equation governs the stability of the origin in the quadratically-damped Mathieu equation, the transition curves of the linear Mathieu equation represent bifurcation curves for the quadratically-damped Mathieu equation (Fig. 1).

Although the linear stability analysis predicts unbounded growth inside the tongues, this is not the case in the non-linear equation (2). Inside the tongues, the non-linear damping in Eq. (2) balances the parametric resonance, leading to the existence of a periodic motion inside the tongues. The method of averaging (see [5]) can be used both to show that periodic motions exist inside the instability tongues, and to obtain an approximation to these periodic motions, valid for small ε . The details of this calculation are given in [4]. These

results predict that at points lying inside the tongue emanating from $\delta = 1/4, \varepsilon = 0$, Eq. (2) exhibits an attractive 2:1 subharmonic motion having period 4π . For this reason the points lying inside this tongue will be referred to as the 2:1 region. Similarly, at points lying inside the tongue emanating from $\delta = 1, \varepsilon = 0$, Eq. (2) is predicted to exhibit a pair of attractive 1:1 periodic motions, each having period 2π . This region will be referred to as the 1:1 region.

3. Numerical determination of the secondary bifurcation

Numerical explorations of the non-linear quadratically-damped Mathieu equation (2) may be accomplished by generating a Poincaré map corresponding to a surface of section $t = 0 \pmod{2\pi}$. Using this technique, a variety of periodic motions are observed, depending upon where we are in the δ - ε parameter plane. Fig. 2 shows schematically the

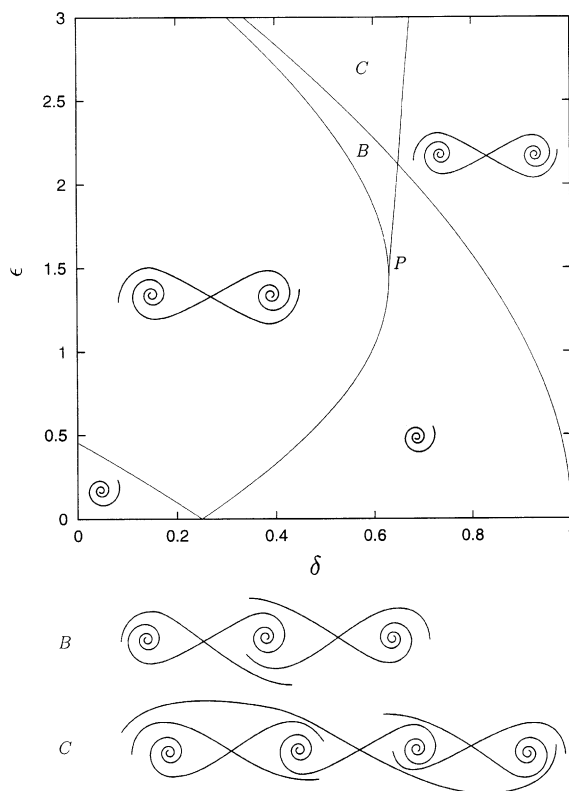


Fig. 2. Phase portraits of the Poincaré Map in the different regions of the parameter plane in the quadratic Mathieu equation.

different Poincaré map portraits that are exhibited by Eq. (2). In these diagrams both stationary and periodic motions appear as fixed points.

We may summarize the features displayed in Fig. 2 as follows: Outside the instability regions, the origin is always stable, as indicated by a lone spiral to the origin. Inside the instability regions, the origin is unstable, as indicated by a saddle-like x at the origin. Inside the 2:1 region the two spiral singularities in the Poincaré map represent a single period 4π motion, whereas in the 1:1 region they represent two period 2π motions. As the transition curves are crossed into the 1:1 region or into the 2:1 region below point P , a supercritical pitchfork bifurcation occurs, and two new stable singular points are created in the Poincaré map, while the origin itself becomes unstable. As the 2:1 region is exited above point P into the region marked B (see Fig. 2), a subcritical pitchfork bifurcation occurs. In this case, the origin becomes stable and an unstable 2:1 subharmonic periodic motion is created. As region B is exited into region C , the 1:1 transition curve is crossed, and the expected supercritical pitchfork bifurcation curve takes place at the origin. The origin once more becomes unstable, while two stable period 2π motions are born out of the origin.

Perhaps the most interesting feature displayed in Fig. 2 corresponds to what happens when we move from either of regions B or C downward across the nearly-straight line bifurcation curve emanating from point P . In this case the two coexisting outermost periodic orbits—the stable and unstable period 4π orbits—coalesce and are destroyed in a saddle-node bifurcation. It is seen that this saddle-node bifurcation does not take place at the origin. *It is the goal of this work to obtain an analytic approximation for this curve on which this secondary bifurcation takes place.*

4. Analytical determination of the secondary bifurcation

In this section, the secondary bifurcation is investigated by a perturbation method applied at the point P . In order to cast Eq. (2) in the proper format, we scale it to

$$\ddot{x} + (\delta + \varepsilon \cos t)x + \mu \dot{x}|x| = 0, \tag{3}$$

where the parameter μ is assumed to be small. We further expand δ and x as follows:

$$x = x_0 + \mu x_1 + \mu^2 x_2 + \mu^3 x_3 + \mu^4 x_4 + \mu^5 x_5 + \dots \tag{4}$$

$$\delta = \delta_0 + \mu \delta_1 + \mu^2 \delta_2 + \mu^3 \delta_3 + \mu^4 \delta_4 + \mu^5 \delta_5 + \dots \tag{5}$$

and further introduce the parameter ε_1 defined by

$$\varepsilon = \varepsilon_0 + \mu \varepsilon_1. \tag{6}$$

We found it necessary to include terms of $\mathcal{O}(\mu^5)$ in Eqs. (4) and (5) in order to get good agreement with numerical simulation. The quantities δ_0 and ε_0 refer to the location of P . The parameter ε_1 measures the deviation of ε from ε_0 at P . Eqs. (3)–(6) represent a perturbation expansion off of the linear Mathieu equation. Because of this, the solution of the unperturbed equation will involve Mathieu functions. The perturbation functions x_i are each required to be periodic.

When Eqs. (4)–(6) are inserted into Eq. (3) and terms are collected in powers of μ , the perturbation equations are

$$Lx_0 = 0, \tag{7}$$

$$Lx_1 = -(\delta_1 + \varepsilon_1 \cos t)x_0 - \frac{dx_0}{dt} \left| \frac{dx_0}{dt} \right|, \tag{8}$$

$$Lx_2 = -\delta_2 x_0 - (\delta_1 + \varepsilon_1 \cos t)x_1 - 2 \frac{dx_1}{dt} \left| \frac{dx_0}{dt} \right|, \tag{9}$$

$$Lx_3 = -\delta_3 x_0 - \delta_2 x_1 - (\delta_1 + \varepsilon_1 \cos t)x_2 - 2 \frac{dx_2}{dt} \left| \frac{dx_0}{dt} \right| - \left(\frac{dx_1}{dt} \right)^2 \operatorname{sgn} \left[\frac{dx_0}{dt} \right], \tag{10}$$

$$Lx_4 = -\delta_4 x_0 - \delta_3 x_1 - \delta_2 x_2 - (\delta_1 + \varepsilon_1 \cos t)x_3 - 2 \frac{dx_3}{dt} \left| \frac{dx_0}{dt} \right| - 2 \operatorname{sgn} \left[\frac{dx_0}{dt} \right] \frac{dx_1}{dt} \frac{dx_2}{dt} - \frac{1}{3} \left(\frac{dx_1}{dt} \right)^3 \delta \left(\frac{dx_0}{dt} \right), \tag{11}$$

$$Lx_5 = -\delta_5 x_0 - \delta_4 x_1 - \delta_3 x_2 - \delta_2 x_3 - (\delta_1 + \varepsilon_1 \cos t)x_4 - 2 \frac{dx_4}{dt} \left| \frac{dx_0}{dt} \right| - 2 \frac{dx_1}{dt} \frac{dx_3}{dt} \operatorname{sgn} \left[\frac{dx_0}{dt} \right]$$

$$\begin{aligned}
 & - \left(\frac{dx_2}{dt} \right)^2 \operatorname{sgn} \left[\frac{dx_0}{dt} \right] \\
 & - \frac{1}{12} \left(\frac{dx_1}{dt} \right)^4 \delta' \left(\frac{dx_0}{dt} \right) \\
 & - \left(\frac{dx_1}{dt} \right)^2 \frac{dx_2}{dt} \delta \left(\frac{dx_0}{dt} \right), \tag{12}
 \end{aligned}$$

where

$$L \equiv \frac{d^2}{dt^2} + (\delta_0 + \varepsilon_0 \cos t) \tag{13}$$

is defined as the Mathieu operator, and where sgn is the signum function and δ is the Dirac- δ function. The signum and Dirac- δ functions arise from the derivatives of the absolute value term in Eq. (3). The details of the foregoing calculations are included in the doctoral thesis of Ramani [6].

The first perturbation equation, Eq. (7), is the linear Mathieu equation. Because P is on the right-hand transition curve of the 2:1 instability tongue, Eq. (7) has as its solution the odd Mathieu function of period 4π [1]. Therefore

$$x_0 = A f_1, \tag{14}$$

where A is a constant that represents the amplitude of a periodic motion, and f_1 denotes the Mathieu function. In this case, the second linearly independent solution of Mathieu’s equation is not used because it is not periodic. In order to simplify what follows we introduce the notational convention that *any function labeled f_i is an odd function, whereas any function labeled g_i is an even function.*

By inserting Eq. (14) into Eq. (8) the following equation for x_1 is obtained

$$Lx_1 = -(\delta_1 + \varepsilon_1 \cos t)A f_1 - A^2 \dot{f}_1 |\dot{f}_1|. \tag{15}$$

Because A represents the amplitude of a motion, it may be thought of as positive. The constant δ_1 is chosen to eliminate secular terms. The secular terms are eliminated by using the Fredholm alternative theorem which states that for a periodic solution to exist for

$$Lx = F, \tag{16}$$

the function F must be orthogonal to the null space of the adjoint operator L^* . In this case, L is self-adjoint, and its null space is spanned by the function f_1 . The

orthogonality condition is expressed as

$$\int_0^{4\pi} f_1 F dt = 0. \tag{17}$$

The Fredholm condition is

$$\begin{aligned}
 \int_0^{4\pi} A f_1 H_1 dt &= - \int_0^{4\pi} (\delta_1 + \varepsilon_1 \cos t) A^2 f_1^2 dt \\
 &- \int_0^{4\pi} A^3 f_1 \dot{f}_1 |\dot{f}_1| dt = 0. \tag{18}
 \end{aligned}$$

The term $-\int_0^{4\pi} (\delta_1 + \varepsilon_1 \cos t) A^2 f_1^2 dt$ in Eq. (18) cannot be further simplified. In the term $-\int_0^{4\pi} A^3 f_1 \dot{f}_1 |\dot{f}_1| dt$, f_1 is an odd function and therefore \dot{f}_1 is an even function. Thus, the integrand in the second term is an odd function that is periodic over an interval of 4π . Since the integral of a periodic odd function over a periodic interval is 0, this term vanishes, leaving

$$\delta_1 \int_0^{4\pi} f_1^2 dt + \varepsilon_1 \int_0^{4\pi} f_1^2 \cos t dt = 0 \tag{19}$$

or

$$\frac{\varepsilon_1}{\delta_1} = - \frac{\int_0^{4\pi} f_1^2 dt}{\int_0^{4\pi} f_1^2 \cos t dt}. \tag{20}$$

However, the only non-linear term in the analysis to this point has vanished without having an effect on the integration. Therefore, the relationship between ε_1 and δ_1 derived in Eq. (20) must also hold for the linear Mathieu equation. The ratio of ε_1 to δ_1 is the local slope of the transition curve near the point $(\delta_0, \varepsilon_0)$. Since P is taken to be the point where the transition curve has infinite slope, this forces $\delta_1 = 0$. From Eq. (20) this is equivalent to requiring

$$\int_0^{4\pi} f_1^2 \cos t dt = 0 \tag{21}$$

at $(\delta_0, \varepsilon_0)$. This requirement provides an analytical condition for $(\delta_0, \varepsilon_0)$, the location of point P on the transition curve.

By substituting $\delta_1 = 0$ back into Eq. (15), the equation on x_1 is now formulated in a solvable way

$$Lx_1 = -\varepsilon_1 A f_1 \cos t - A^2 \dot{f}_1 |\dot{f}_1|. \tag{22}$$

The first term on the right-hand side of Eq. (22) is an odd term, whereas the second term is an even term. By linearity these may be treated independently, and the sum of their individual particular solutions may be

used to solve the full equation. Therefore, the functions f_2 and g_1 are defined by

$$Lf_2 = -f_1 \cos t \tag{23}$$

$$Lg_1 = -\dot{f}_1 |\dot{f}_1|. \tag{24}$$

The solution to the full Eq. (22) is then

$$x_1 = A\varepsilon_1 f_2 + A^2 g_1. \tag{25}$$

For the most general periodic solution, an arbitrary multiple of f_1 could be added to the solution for x_1 . In fact, because $Lf_1 = 0$, arbitrary multiples of f_1 could be added to any of the odd functions that arise from the perturbation method. However, we show in Appendix A that the results of the method are independent of the addition of multiples of f_1 . Moreover, any such solutions of the homogeneous problem could be absorbed into x_0 , representing a change in initial conditions. Therefore, no multiple of f_1 will be added to any of the solutions, in order to ease the algebra. Note that an arbitrary multiple of f_1 cannot be added to any of the g_i . This is because the g_i are required to be even functions. This property would be destroyed by adding multiples of the odd function f_1 .

By continuing in a similar fashion, the second Fredholm condition becomes

$$\begin{aligned} A^2 \delta_2 \int_0^{4\pi} f_1^2 dt + A^2 \varepsilon_1^2 \int_0^{4\pi} f_1 f_2 \cos t dt \\ + A^3 \varepsilon_1 \int_0^{4\pi} f_1 (g_1 \cos t + 2\dot{f}_2 |\dot{f}_1|) dt \\ + 2A^4 \int_0^{4\pi} f_1 |\dot{f}_1| \dot{g}_1 dt = 0, \end{aligned} \tag{26}$$

which can be solved to yield

$$\begin{aligned} \delta_2 = -\varepsilon_1^2 \frac{\int_0^{4\pi} f_1 f_2 \cos t dt}{\int_0^{4\pi} f_1^2 dt} - 2A^2 \frac{\int_0^{4\pi} f_1 |\dot{f}_1| \dot{g}_1 dt}{\int_0^{4\pi} f_1^2 dt} \\ \equiv k_1 \varepsilon_1^2 + 2k_2 A^2, \end{aligned} \tag{27}$$

where

$$k_1 = -\frac{\int_0^{4\pi} f_1 f_2 \cos t dt}{\int_0^{4\pi} f_1^2 dt} \tag{28}$$

$$k_2 = -\frac{\int_0^{4\pi} f_1 |\dot{f}_1| \dot{g}_1 dt}{\int_0^{4\pi} f_1^2 dt} \tag{29}$$

are constants that need to be computed numerically.

Substituting Eq. (27) back into the last of Eq. (9), a new equation on x_2 is obtained:

$$\begin{aligned} Lx_2 = -A\varepsilon_1^2 (k_1 f_1 + f_2 \cos t) \\ -A^2 \varepsilon_1 (g_1 \cos t + 2\dot{f}_2 |\dot{f}_1|) \\ -2A^3 (k_2 f_1 + |\dot{f}_1| \dot{g}_1). \end{aligned} \tag{30}$$

Each of the three terms on the right-hand side of (30) is either even or odd, and so the solution for x_2 consists of three terms

$$x_2 = A\varepsilon_1^2 f_3 + A^2 \varepsilon_1 g_2 + 2A^3 f_4, \tag{31}$$

where

$$Lf_3 = -k_1 f_1 - f_2 \cos t, \tag{32}$$

$$Lg_2 = -g_1 \cos t - 2\dot{f}_2 |\dot{f}_1|, \tag{33}$$

$$Lf_4 = -k_2 f_1 - \dot{g}_1 |\dot{f}_1|. \tag{34}$$

This procedure is continued at each higher order of μ . At each stage, the latest δ_i is obtained from the Fredholm condition. Using δ_i , the differential equation on x_i is solved. At each stage, we encounter certain integrals which we leave in unevaluated form and abbreviate by using the notation k_i as above. The bifurcation curve is determined by the values of δ_i and k_i . For that reason, they are given here. The definitions of the auxiliary functions f_i and g_i as well as the solutions to Eqs. (7)–(11) are given in Appendix B.

The δ_i are

$$\delta_1 = 0, \tag{35}$$

$$\delta_2 = k_1 \varepsilon_1^2 + 2k_2 A^2, \tag{36}$$

$$\delta_3 = k_3 \varepsilon_1^3 + k_4 A^2 \varepsilon_1, \tag{37}$$

$$\delta_4 = k_5 A^4 + k_6 A^2 \varepsilon_1^2 + k_7 \varepsilon_1^4, \tag{38}$$

$$\begin{aligned} \delta_5 = \varepsilon_1^5 k_8 + A^2 \varepsilon_1^3 k_9 + A^3 \varepsilon_1^3 k_{10} + A^4 \varepsilon_1 k_{11} \\ + A^4 \varepsilon_1^3 k_{12} + A^5 \varepsilon_1 k_{13} + A^6 \varepsilon_1 k_{14}, \end{aligned} \tag{39}$$

where

$$k_1 = -\frac{\int_0^{4\pi} f_1 f_2 \cos t dt}{\int_0^{4\pi} f_1^2 dt}, \tag{40}$$

$$k_2 = -\frac{\int_0^{4\pi} f_1 \dot{g}_1 |\dot{f}_1| dt}{\int_0^{4\pi} f_1^2 dt}, \tag{41}$$

$$k_3 = -\frac{\int_0^{4\pi} k_1 f_1 f_2 + f_1 f_3 \cos t \, dt}{\int_0^{4\pi} f_1^2 \, dt}, \tag{42}$$

$$k_4 = -\frac{\int_0^{4\pi} 2k_2 f_1 f_2 + 2f_1 f_4 \cos t + 2f_1 g_2 |\dot{f}_1| \, dt}{\int_0^{4\pi} f_1^2 \, dt} - \frac{\int_0^{4\pi} 2f_1 \dot{f}_2 g_1 \operatorname{sgn} \dot{f}_1 \, dt}{\int_0^{4\pi} f_1^2 \, dt}, \tag{43}$$

$$k_5 = -\frac{\int_0^{4\pi} 4k_2 f_1 f_4 + 4f_1 \dot{f}_4 g_1 \operatorname{sgn} \dot{f}_1 + 2f_1 g_4 |\dot{f}_1| \, dt}{\int_0^{4\pi} f_1^2 \, dt}, \tag{44}$$

$$k_6 = -\frac{\int_0^{4\pi} 2f_1 \dot{f}_3 g_1 \operatorname{sgn} \dot{f}_1 + 2f_1 \dot{f}_2 g_2 \operatorname{sgn} \dot{f}_1 \, dt}{\int_0^{4\pi} f_1^2 \, dt} - \frac{\int_0^{4\pi} 2f_1 g_3 |\dot{f}_1| + 2k_1 f_1 f_4 + 2k_2 f_1 f_3 \, dt}{\int_0^{4\pi} f_1^2 \, dt} - \frac{\int_0^{4\pi} k_4 f_1 f_2 + f_1 f_5 \cos t \, dt}{\int_0^{4\pi} f_1^2 \, dt}, \tag{45}$$

$$k_7 = -\frac{\int_0^{4\pi} k_1 f_1 f_3 + f_1 f_6 \cos t + k_3 f_1 f_2 \, dt}{\int_0^{4\pi} f_1^2 \, dt}, \tag{46}$$

$$k_8 = -\frac{\int_0^{4\pi} f_1(k_7 f_2 + k_3 f_3 + k_1 f_6 + f_7 \cos t) \, dt}{\int_0^{4\pi} f_1^2 \, dt}, \tag{47}$$

$$k_9 = -\frac{\int_0^{4\pi} f_1(k_6 f_2 + k_4 f_3 + 2k_3 f_4 + 2k_2 f_6) \, dt}{\int_0^{4\pi} f_1^2 \, dt} - \frac{\int_0^{4\pi} f_1(k_5 f_5 + 2g_5 |\dot{f}_1|) \, dt}{\int_0^{4\pi} f_1^2 \, dt} - \frac{\int_0^{4\pi} f_1(2\dot{f}_2 g_3 \operatorname{sgn} \dot{f}_1 + 2\dot{f}_3 g_2 \operatorname{sgn} \dot{f}_1) \, dt}{\int_0^{4\pi} f_1^2 \, dt} - \frac{\int_0^{4\pi} f_1(2\dot{f}_6 g_1 \operatorname{sgn} \dot{f}_1 + f_8 \cos t) \, dt}{\int_0^{4\pi} f_1^2 \, dt}, \tag{48}$$

$$k_{10} = -\frac{2}{3} \frac{\int_0^{4\pi} f_1(\dot{g}_7 |\dot{f}_1| + f_{11} \cos t) \, dt}{\int_0^{4\pi} f_1^2 \, dt}, \tag{49}$$

$$k_{11} = -\frac{\int_0^{4\pi} f_1(k_5 f_2 + 2k_4 f_4 + 2k_2 f_5) \, dt}{\int_0^{4\pi} f_1^2 \, dt} - \frac{\int_0^{4\pi} f_1(2\dot{g}_6 |\dot{f}_1| + 2\dot{f}_2 g_4 \operatorname{sgn} \dot{f}_1) \, dt}{\int_0^{4\pi} f_1^2 \, dt} - \frac{\int_0^{4\pi} f_1(4\dot{f}_4 g_2 \operatorname{sgn} \dot{f}_1 + 2\dot{f}_5 g_1 \operatorname{sgn} \dot{f}_1 + f_9 \cos t) \, dt}{\int_0^{4\pi} f_1^2 \, dt}, \tag{50}$$

$$k_{12} = -\frac{1}{3} \frac{\int_0^{4\pi} f_1 \dot{f}_2^3 g_1 \delta'(f_1) \, dt}{\int_0^{4\pi} f_1^2 \, dt}, \tag{51}$$

$$k_{13} = -\frac{\int_0^{4\pi} f_1(2\dot{g}_8 |\dot{f}_1| + \frac{1}{3} f_{10} \cos t) \, dt}{\int_0^{4\pi} f_1^2 \, dt} \tag{52}$$

$$k_{14} = -\frac{1}{3} \frac{\int_0^{4\pi} f_1 \dot{f}_2 \dot{g}_1^3 \delta'(f_1) \, dt}{\int_0^{4\pi} f_1^2 \, dt}. \tag{53}$$

Numerical solution of the perturbation Eqs. (7)–(11) yields the functions f_i and g_i (see Appendix B) and then the values of the k_i may be found by numerical quadrature, see Table 1. Because the f_i and the g_i are required to be periodic functions, their initial conditions need to be chosen carefully. A shooting procedure was used first to locate δ_0 and ε_0 , and then to obtain the initial conditions for the g_i . The shooting method returned $\delta_0 = 0.630420248517023$ and $\varepsilon_0 = 1.438618533234416$ in double precision, in agreement with values obtained by direct numerical integration of Eq. (2).

Table 1
Values of k_i

k_1	-0.176795720204351	k_8	-0.005343518899145
k_2	0.000449147391502	k_9	0.041196711700806
k_3	0.023845390107660	k_{10}	0.000000000000001
k_4	0.059627911982873	k_{11}	0.243420338228478
k_5	0.008051597731526	k_{12}	0.024121956135593
k_6	0.133978124987812	k_{13}	0.000000000000000
k_7	0.008726800055536	k_{14}	0.003191162023248

Substituting Eqs. (35)–(39) into Eq. (5), the following expression for δ is obtained:

$$\begin{aligned} \delta = & \delta_0 + \varepsilon_1 k_{14} A^6 + (\varepsilon_1 k_{11} + \varepsilon_1^3 k_{12} + k_5) A^4 \\ & + (2k_2 + k_4 \varepsilon_1 + k_6 \varepsilon_1^2 + k_9 \varepsilon_1^3) A^2 \\ & + (k_1 \varepsilon_1^2 + k_3 \varepsilon_1^3 + k_7 \varepsilon_1^4 + k_8 \varepsilon_1^5). \end{aligned} \quad (54)$$

This equation relates a given value of δ and ε_1 to the predicted amplitude A of the newly bifurcated unstable 2:1 subharmonic 4π -periodic orbit. As a check on all the perturbation calculations, we may use this equation to generate a value of A with which we may compare the perturbation expression for $x(t)$, that is, Eq. (4) supplemented by the expressions in Appendix B and the values of the k_i in Table 1, with the results of direct numerical integration of Eq. (2). To obtain a comparison, a method of numerically generating the unstable orbit is needed. This can be done by starting the integration near the stable manifold of the unstable orbit. If the initial condition is close enough to the stable manifold, the system will spend enough time near the unstable orbit to obtain a good approximation of it. The stable manifold was found by a bisection method, and involved choosing an appropriate initial condition accurate to 16 significant figures.

Figs. 3 and 4 offer a comparison between the predicted unstable periodic orbit obtained from the perturbation method (dashed) and from numerical integration (solid) for $\delta = 0.6305$ and $\varepsilon = 1.47$. For these values of the parameters, Eq. (54) predicts $A \approx 0.2542$. Fig. 3 shows a phase portrait of the system, while Fig. 4 shows the time history of the system. For these values of δ and ε , the agreement between the analytical approximation and the numerical integration is quite good. For comparison, the location of P was determined to be about $\delta_0 \approx 0.6304$ and $\varepsilon_0 \approx 1.4386$.

As the value of δ is increased away from the transition curve and towards the secondary bifurcation curve, the agreement between the analytical and numerical solutions worsens. Fig. 5 and 6 show the approximations for $\delta = 0.631$ and $\varepsilon = 1.47$, with the bifurcation point P located at $\delta_0 \approx 0.6304$ and $\varepsilon_0 \approx 1.4386$. Despite the small change in δ there is a marked change in the agreement. These figures suggest that the power series may not converge close to the bifurcation curve. The lack of accuracy could be due to either the number of terms taken being too

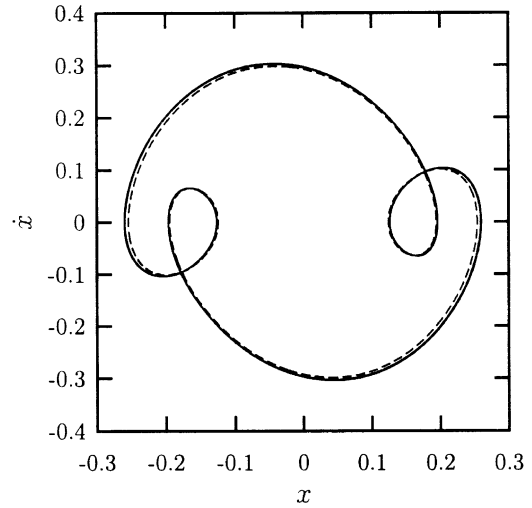


Fig. 3. Comparison of numerical and analytical approximations of the unstable periodic orbit in the phase plane. Analytical approximation is dashed, numerical integration is solid. Here $\delta = 0.6305$, $\varepsilon = 1.47$ and $A = 0.2542$. $\delta_0 \approx 0.6304$ and $\varepsilon_0 \approx 1.4386$.

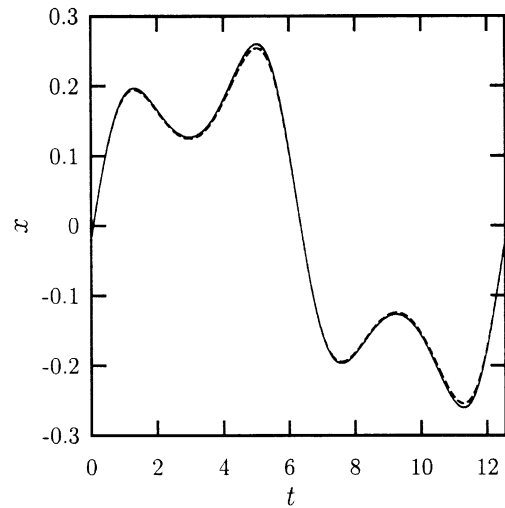


Fig. 4. Comparison of numerical and analytical approximations of the unstable periodic orbit as a time history. Analytical approximation is dashed, numerical integration is solid. Here $\delta = 0.6305$, $\varepsilon = 1.47$ and $A = 0.2542$. $\delta_0 \approx 0.6304$ and $\varepsilon_0 \approx 1.4386$.

small or the radius of convergence of the series not being large enough to reach the bifurcation curve. In the former case, more terms could be added, but the computational difficulties increase considerably

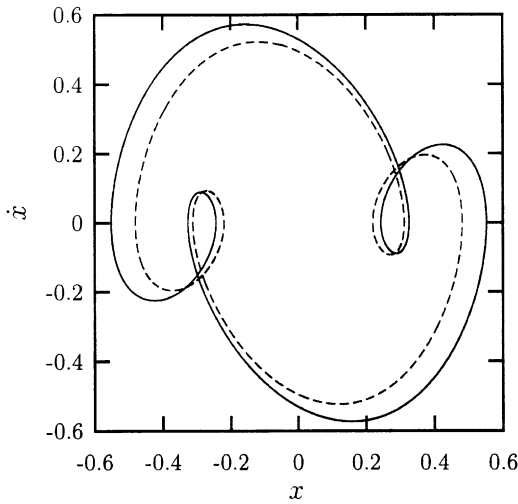


Fig. 5. Comparison of numerical and analytical approximations of the unstable periodic orbit in the phase plane. Analytical approximation is dashed, numerical integration is solid. Here $\delta = 0.631$, $\varepsilon = 1.47$ and $A = 0.3811$. $\delta_0 \approx 0.6304$ and $\varepsilon_0 \approx 1.4386$.

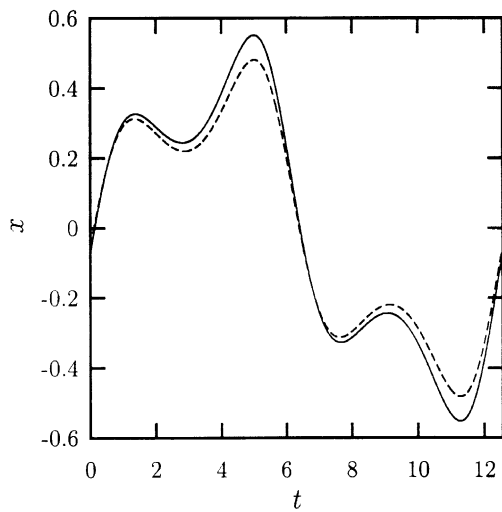


Fig. 6. Comparison of numerical and analytical approximations of the unstable periodic orbit as a time history. Analytical approximation is dashed, numerical integration is solid. Here $\delta = 0.631$, $\varepsilon = 1.47$ and $A = 0.3811$. $\delta_0 \approx 0.6304$ and $\varepsilon_0 \approx 1.4386$.

with each step. In the latter case, the power series expansion will not give reasonable agreement near the bifurcation curve, no matter how many terms are taken.

With these convergence problems in mind, we now proceed to attempt to obtain an analytical expression for the secondary bifurcation curve. We begin by setting up a convenient local coordinate system in parameter space centered at point P , as follows: Note that in Eq. (54), the periodic motion has an amplitude A which approaches 0 as we approach the bifurcation point. This bifurcation occurs along the transition curve. Therefore, by setting $A = 0$ an expression for the transition curve can be obtained. A natural choice of coordinates is suggested by this observation. The new coordinates are defined by

$$u = \Delta - (k_1\varepsilon_1^2 + k_3\varepsilon_1^3 + k_7\varepsilon_1^4 + k_8\varepsilon_1^5), \tag{55}$$

$$v = \varepsilon_1, \tag{56}$$

where $\Delta \equiv \delta - \delta_0$. The coordinate u measures the distance in δ from the transition curve. The coordinate v measures the distance in ε from P .

In the new coordinates, Eq. (54) takes the form

$$u = vk_{14}A^6 + (vk_{11} + v^3k_{12} + k_5)A^4 + (2k_2 + k_4v + k_6v^2 + k_9v^3)A^2. \tag{57}$$

The secondary bifurcation curve can be obtained by noting that Eq. (57) generates a series expansion for u in terms of v for small values of A . If the value of v is fixed—equivalently, if the value of ε_1 is fixed—then Eq. (57) can be considered to give the value of A as the value of u is varied. Since u is a measure of the distance from the transition curve, this curve gives the dependence of A on δ . For a given value of u there should be two real, positive values of A , corresponding to the two periodic motions (one stable and one unstable) that exist in this region of the parameter plane. The bifurcation occurs when these two motions come together. In terms of the u - A curve, this happens at a vertical tangency in the curve, or when $du/dA = 0$. This condition, along with Eq. (57), gives two conditions on u , v , and A . A can be eliminated from these equations, resulting in a single equation between u and v .

Because of the slow convergence of the series in Eq. (57), illustrated by Figs. 3 and 4 and Figs. 5 and 6, directly following the prescription above will not yield the bifurcation curve. Even assuming that the radius of convergence of the series will allow extension to the bifurcation curve, a prohibitive number of terms

may be needed to actually obtain satisfactory convergence. To improve the convergence properties of the power series, Padé approximants are used. The theory of Padé approximants is discussed in [5,7]. The fundamental idea of Padé summation is to replace a truncated power series by a rational function of polynomials, which has the same Taylor series as the truncated power series.

To apply the method to this problem, Eq. (57) is converted to a Padé approximant. For this case, there are three possible approximants

$$u = a^3 b_3 + a^2 b_2 + a b_1, \tag{58}$$

$$u = \frac{-ab_1^3}{a^2(b_1 b_3 - b_2^2) + ab_1 b_2 - b_1^2}, \tag{59}$$

$$u = \frac{a^2(b_1 b_3 - b_2^2) - ab_1 b_2}{ab_3 - b_1}, \tag{60}$$

where $a = A^2$, and

$$b_1 = 2k_2 + k_4 v + k_6 v^2 + k_9 v^3, \tag{61}$$

$$b_2 = vk_{11} + v^3 k_{12} + k_5, \tag{62}$$

$$b_3 = vk_{14}. \tag{63}$$

Each of the three approximants needs to be tested individually for good convergence. Of the three, only Eq. (59) gives adequate convergence results. By taking the derivative of Eq. (59) with respect to a and then eliminating a , substituting the values of the b_i and then the k_i , the following numerical equation relating u and v can be obtained

$$u = 0.01465v + 0.06596v^2. \tag{64}$$

Eq. (64) can be written in terms of δ and ε by substituting Eq. (55). Finally, a relationship between δ and ε may be obtained

$$\delta = -0.00534\varepsilon^5 + 0.04716\varepsilon^4 - 0.13696\varepsilon^3 + 0.14908\varepsilon^2 + 0.01551\varepsilon + 0.58301. \tag{65}$$

Eq. (65) is an approximation to the secondary bifurcation curve.

Fig. 7 shows the analytical and numerical approximations to the bifurcation curve. The analytical approximation, shown as a solid line, is in close

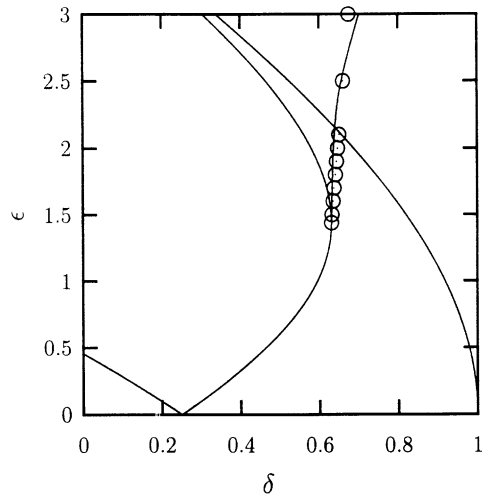


Fig. 7. Comparison of analytical and numerical approximation to the secondary bifurcation curve. Analytical approximation is the solid line, numerical values are points.

agreement up to $\varepsilon = 2.5$, at which point it becomes less reliable. The perturbation method is assumed to be valid in the neighborhood of $\varepsilon_0 \approx 1.4386$, so the approximation in Eq. (65) is working quite well.

In cases such as the present one, it seems that the bifurcation curve should arise from a tangency with the transition curve. Since the bifurcation is assumed to occur at a point along the transition curve which has a vertical tangency, the bifurcation curve itself is assumed to have a vertical tangency. In the present instance, this is not the case. The analytical expression for the bifurcation curve is nearly vertical, but it is not truly vertical.

5. Conclusions

The bifurcations in the quadratically-damped Mathieu equation were studied. Special focus was given to the region of the δ - ε parameter plane around point P , the point of infinite slope along the right transition curve of the 2:1 instability region. In this region a bifurcation sequence was numerically identified. It was observed that above P an unstable periodic motion is born by crossing out of the instability region. On the other hand, below P , a stable periodic motion

is born by crossing into the instability region. Moreover, a secondary bifurcation curve in which the previously mentioned stable and unstable periodic motions merge, was seen to emanate from point P .

In order to obtain an approximation for this secondary bifurcation, a new approach was developed. This involved perturbing directly off of Mathieu's equation and using Mathieu functions instead of the usual sines and cosines. An interesting feature of this method is its semi-analytical nature. Because Mathieu functions do not have closed-form representations that are easy to manipulate, the method needed to be executed semi-analytically, that is, certain integrals had to be evaluated by numerical quadrature.

When combined with Padé approximants, the perturbation method recovered an acceptable approximation to the secondary bifurcation curve in a neighborhood of point P . In fact, the resulting approximation was seen to be reasonable for values of ε up to 2.5. However, since the perturbation method itself can be expected to be valid only in a neighborhood of point P , this agreement must be viewed as serendipitous.

Acknowledgements

Author Ramani wishes to acknowledge support for this work in the form of a National Science Foundation Graduate Research Fellowship. This work was partially supported by the Office of Naval Research, Program Officer Dr. Roy Elswick, Code 321.

Appendix A. Invariance of the k_i

The solution to the perturbation equations, and thus the predictions of the method, depend on the values of the detuning parameters, δ_i , which in turn depend on the constants k_i . In the solution of the perturbation equations it was mentioned that arbitrary multiples of f_1 could be added to any odd function and to any of the x_i . The purpose of this section is to demonstrate that the k_i , and therefore the results of the method, are not affected by addition of multiples of f_1 .

Theorem 1. Consider the functions f_i , their corresponding constants k_i , and the new functions \tilde{f}_i

defined by

$$\tilde{f}_i = c_i f_i + f_i \quad (\text{A.1})$$

and their corresponding constants \tilde{k}_i . For arbitrary choice of c_i

$$\tilde{k}_i = k_i. \quad (\text{A.2})$$

Proof. The proof of this theorem is obtained by direct computation of the \tilde{k}_i . Suppose that A has been chosen and that $x_0 = A f_1$. Then $L f_2 = -f_1 \cos t$. Now, define

$$\tilde{f}_2 = c_2 f_1 + f_2. \quad (\text{A.3})$$

From Eq. (28)

$$\begin{aligned} \tilde{k}_1 &= -\frac{\int_0^{4\pi} f_1 \tilde{f}_2 \cos t \, dt}{\int_0^{4\pi} f_1^2 \, dt} \\ &= -\frac{\int_0^{4\pi} f_1 (f_2 + c_2 f_1) \cos t \, dt}{\int_0^{4\pi} f_1^2 \, dt}. \end{aligned} \quad (\text{A.4})$$

Since the denominators of all the k_i are identical and do not vary they will be ignored from now on. Expanding the numerator gives

$$\begin{aligned} \tilde{k}_1 \int_0^{4\pi} f_1^2 \, dt &= -\int_0^{4\pi} f_1 f_2 \cos t \, dt \\ &\quad -c_2 \int_0^{4\pi} f_1^2 \cos t \, dt. \end{aligned} \quad (\text{A.5})$$

The first term on the right-hand side is the numerator of k_1 . The second term on the right-hand side gives zero as a result of the first Fredholm condition, Eq. (21). Therefore, $\tilde{k}_1 = k_1$.

Because k_2 depends on f_1 and g_1 , it is not affected by addition of f_1 , and is therefore invariant.

The situation becomes increasingly complicated for the other k_i . From Eq. (42)

$$k_3 = -\frac{\int_0^{4\pi} f_1 (k_1 f_2 + f_3 \cos t) \, dt}{\int_0^{4\pi} f_1^2 \, dt}. \quad (\text{A.6})$$

To see how k_3 is affected, it is first necessary to determine how f_3 is affected. From the definition of f_3

$$\begin{aligned} L \tilde{f}_3 &= k_1 f_1 - \tilde{f}_2 \cos t \\ &= k_1 f_1 - (f_2 + c_2 f_1) \cos t. \end{aligned} \quad (\text{A.7})$$

Expanding this even further

$$L\tilde{f}_3 = -k_1 f_1 - f_2 \cos t - c_2 f_1 \cos t. \tag{A.8}$$

The first two terms of the equation give the original definition of f_3 . The last term of the equation will give rise to f_2 , from Eq. (23). Thus,

$$\tilde{f}_3 = f_3 + c_2 f_2 + c_3 f_1 \tag{A.9}$$

and

$$\tilde{k}_3 \int_0^{4\pi} f_1^2 dt = - \int_0^{4\pi} f_1 (k_1 \tilde{f}_2 + \tilde{f}_3 \cos t) dt. \tag{A.10}$$

Expanding this again

$$\begin{aligned} \tilde{k}_3 \int_0^{4\pi} f_1^2 dt &= - \int_0^{4\pi} k_1 f_1 (f_2 + c_2 f_1) dt - \int_0^{4\pi} f_1 \cos t \\ &\quad \times (f_3 + c_2 f_2 + c_3 f_1) dt. \end{aligned} \tag{A.11}$$

Collecting terms in the c_i yields

$$\begin{aligned} \tilde{k}_3 \int_0^{4\pi} f_1^2 dt &= - \int_0^{4\pi} f_1 (k_1 f_2 + f_3 \cos t) dt \\ &\quad - c_3 \int_0^{4\pi} f_1^2 \cos t dt \\ &\quad - c_2 \int_0^{4\pi} (k_1 f_1^2 + f_1 f_2 \cos t) dt. \end{aligned} \tag{A.12}$$

The first term on the right-hand side is the numerator of k_3 . The second term on the right-hand side is zero by Eq. (21). In the last term, $k_1 \int_0^{4\pi} f_1^2 dt = - \int_0^{4\pi} f_1 f_2 \cos t dt$, by Eq. (28). Therefore the last term vanishes, leaving $\tilde{k}_3 = k_3$.

This computation can be carried out for all of the k_i in a similar manner.

Appendix B. Definitions of f_i and g_i

In this appendix we present definitions for the functions in the perturbation method at point P . The method for developing these is given

in the text.

$$x_0 = A f_1, \tag{B.1}$$

$$x_1 = A \varepsilon_1 f_2 + A^2 g_1, \tag{B.2}$$

$$x_2 = A \varepsilon_1^2 f_3 + A^2 \varepsilon_1 g_2 + 2A^3 f_4, \tag{B.3}$$

$$x_3 = A^2 \varepsilon_1^2 g_3 + A^4 g_4 + A^3 \varepsilon_1 f_5 + A \varepsilon_1^3 f_6, \tag{B.4}$$

$$\begin{aligned} x_4 &= A \varepsilon_1^4 f_7 + A^2 \varepsilon_1^3 g_5 + A^3 \varepsilon_1^2 f_8 + A^4 \varepsilon_1 g_6 \\ &\quad + A^5 f_9 + \frac{A^6}{3} f_{10} + \frac{A^3 \varepsilon_1^3}{3} g_7 + A^4 \varepsilon_1^2 f_{11} + A^5 \varepsilon_1 g_8, \end{aligned} \tag{B.5}$$

where

$$L f_1 = 0, \tag{B.6}$$

$$L f_2 = -f_1 \cos t, \tag{B.7}$$

$$L f_3 = -k_1 f_1 - f_2 \cos t, \tag{B.8}$$

$$L f_4 = -k_2 f_1 - \dot{g}_1 |f_1|, \tag{B.9}$$

$$\begin{aligned} L f_5 &= -k_4 f_1 - 2k_2 f_2 - 2f_4 \cos t \\ &\quad - 2\dot{g}_2 |f_1| - 2f_2 \dot{g}_1 \operatorname{sgn} \dot{f}_1, \end{aligned} \tag{B.10}$$

$$L f_6 = -k_3 f_1 - k_1 f_2 - f_3 \cos t, \tag{B.11}$$

$$L f_7 = -k_7 f_1 - k_3 f_2 - k_1 f_3 - f_6 \cos t, \tag{B.12}$$

$$\begin{aligned} L f_8 &= -k_6 f_1 - k_4 f_2 - 2k_2 f_3 - 2k_1 f_4 - 2\dot{g}_3 |f_1| \\ &\quad - 2\dot{g}_2 \dot{f}_2 \operatorname{sgn} \dot{f}_1 - 2\dot{g}_1 \dot{f}_3 \operatorname{sgn} \dot{f}_1 - f_5 \cos t, \end{aligned} \tag{B.13}$$

$$\begin{aligned} L f_9 &= -k_5 f_1 - 4k_2 f_4 - 2\dot{g}_4 |f_1| - 4\dot{g}_1 \dot{f}_4 \operatorname{sgn} \dot{f}_1, \end{aligned} \tag{B.14}$$

$$L f_{10} = -\dot{f}_2^3 \delta(A f_1), \tag{B.15}$$

$$L f_{11} = -\dot{g}_1^2 \dot{f}_2 \delta(A f_1), \tag{B.16}$$

$$L g_1 = -\dot{f}_1 |f_1|, \tag{B.17}$$

$$L g_2 = -g_1 \cos t - 2\dot{f}_2 |f_1|, \tag{B.18}$$

$$Lg_3 = -k_1g_1 - g_2 \cos t - 2\dot{f}_3|\dot{f}_1| - \dot{f}_2^2 \operatorname{sgn} \dot{f}_1, \quad (\text{B.19})$$

$$Lg_4 = -2k_2g_1 - 4\dot{f}_4|\dot{f}_1| - \dot{g}_1^2 \operatorname{sgn} \dot{f}_1, \quad (\text{B.20})$$

$$Lg_5 = -k_3g_1 - k_1g_2 - g_3 \cos t - 2\dot{f}_6|\dot{f}_1| - 2\dot{f}_2\dot{f}_3 \operatorname{sgn} \dot{f}_1, \quad (\text{B.21})$$

$$Lg_6 = -k_4g_1 - 2k_2g_2 - g_4 \cos t - 2\dot{g}_2\dot{g}_1 \operatorname{sgn} \dot{f}_1 - 2\dot{f}_5|\dot{f}_1| - 4\dot{f}_4\dot{f}_2 \operatorname{sgn} \dot{f}_1, \quad (\text{B.22})$$

$$Lg_7 = -\dot{g}_1^3 \delta(A\dot{f}_1), \quad (\text{B.23})$$

$$Lg_8 = -\dot{g}_1\dot{f}_2^2 \delta(A\dot{f}_1). \quad (\text{B.24})$$

References

- [1] J. Stoker, *Nonlinear Vibrations*, Wiley-Interscience, New York, 1950.
- [2] A.H. Nayfeh, D.T. Mook, *Nonlinear Oscillations*, Wiley, New York, 1979.
- [3] R.H. Rand, D.V. Ramani, W.L. Keith, K.M. Cipolla, Theoretical study of a submarine towed-array lifting device, in: *Proceedings of the UDT (Undersea Defence Technology) Europe 2000 Conference (CD-ROM)*, June 27–29, 2000, Wembley Conference Center, London, UK, June 2000.
- [4] R.H. Rand, D.V. Ramani, W.L. Keith, K.M. Cipolla, The Quadratically Damped Mathieu Equation and its Application to Submarine Dynamics in: *Control of Noise and Vibration: New Millennium*, AD-Vol. 61, November 5–10, 2000, Orlando, FL, ASME, New York, November 2000, pp. 39–50.
- [5] R.H. Rand, *Topics in Nonlinear Dynamics with Computer Algebra*, Gordon and Breach Science Publishers, USA, 1994.
- [6] D.V. Ramani, *The Nonlinear Dynamics of Towed Array Lifting Devices*, Ph.D. Thesis, Cornell University, Ithaca, NY, 2001.
- [7] C.M. Bender, S.A. Orszag, *Advanced Mathematical Methods For Scientists and Engineers*, McGraw-Hill, Inc., New York, 1978.